Running head: Description of *Hemiarma marina* n. g., n. sp.

A New Heterotrophic Cryptomonad: *Hemiarma marina* n. g., n. sp.

Takashi Shiratori[a] and Ken-ichiro Ishida[b]

a Graduate School of Life and Environmental Sciences, University of Tsukuba, Tsukuba, Ibaraki 305-8572, Japan

b Faculty of Life and Environmental Sciences, University of Tsukuba, Tsukuba, Ibaraki 305-8572, Japan

Correspondence

T. Shiratori, Graduate School of Life and Environmental Sciences, University of Tsukuba, 1-1-1, Tennoudai, Tsukuba, Ibaraki 305-8572, Japan

Telephone number: +81 298 53 4533;

FAX number: +81 298 53 4533;

e-mail: wb.takashi@gmail.com

ABSTRACT

We report a new heterotrophic cryptomonad *Hemiarma marina* n. g., n. sp. that was collected from a seaweed sample from the Republic of Palau. In our molecular phylogenetic analyses using the small subunit ribosomal RNA gene, *H. marina* formed a clade with two marine environmental sequences, and the clade was placed as a sister lineage of the freshwater cryptomonad environmental clade CRY1. Alternatively, in the concatenated large and small subunit ribosomal RNA gene phylogeny, *H. marina* was placed as a sister lineage of *Goniomonas*. Light and electron microscopic observations showed that *H. marina* shares several ultrastructural features with cryptomonads, such as flattened mitochondrial cristae, a periplast cell covering, and ejectisomes that consist of two coiled ribbon structures. On the other hand, *H. marina* exhibited unique behaviors, such as attaching to substrates with its posterior flagellum and displaying a jumping motion. *H. marina* also had unique periplast arrangement and flagellar transitional region. On the basis of both molecular and morphological information, we concluded that *H. marina* should be treated as new genus and species of cryptomonads.

Keywords

Cryptista; Cryptophyceae; environmental sequences; molecular phylogeny; SSU rRNA; ultrastructure

INTRODUCTION

Cryptomonads (or Cryptomonada) are an assemblage of unicellular photosynthetic and heterotrophic flagellates that are widely distributed in marine and freshwater environments (Clay et al. 1999; Gillott 1990; Kugrens et al. 2002). Cryptomonads are characterized by an asymmetric and compressed cell shape, mitochondria with flat cristae, a specific cell

covering that is called periplast, ejectisomes with two coiled ribbon components, and a transitional region with two or more septa (Gillott 1990; Kugrens et al. 2002). Cryptomonads are separated into two classes, the Cryptophyceae and the Goniomonadea. Members of the Cryptophyceae possess plastids that are enclosed by four envelope membranes and are derived from a red alga. Furthermore, the plastids retain a remnant nucleus of the red alga (nucleomorph) in a space between the outer two and inner two membranes (Archibald and Keeling 2002; Graham et al. 2009; Kugrens et al. 2002). Although most cryptophyceans are photosynthetic or mixotrophic, the species *Cryptomonas paramecium* is known to be exclusively heterotrophic and possesses colorless plastids (leucoplasts) with four envelope membranes and a nucleomorph (Heywood 1988; Sepsenwol 1973). Alternatively, Goniomonadea consists of the single genus *Goniomonas,* which is a group of phagotrophic flagellates that lacks plastids. In addition to the absence of plastids, *Goniomonas* differs from cryptophyceans in having an extremely flattened cell body and large rectangular periplast plates (Hill 1991; Martin-Cereceda et al. 2010).

Previous molecular phylogenetic analyses revealed that cryptomonads are positioned as sister to the kathablepharids, which is an assemblage of eukaryote-eating flagellates (Okamoto and Inouye 2005). Katablepharids possess different ultrastructural features from those of cryptomonads, such as mitochondria with tubular cristae, a bilayered sheath as a cell covering, a conoid-like feeding apparatus, and a single septum in the flagellar transitional region (Clay and Kugrens 1999; Okamoto and Inouye 2005, 2006). Katablepharids and cryptomonads both possess similar ejectisomes that contain coiled ribbon structures; however, those of the katablepharids contain a single coiled ribbon structure, whereas those of cryptomonads contain two (Clay and Kugrens 1999; Kugrens et al. 2002). Recent environmental DNA surveys of small subunit ribosomal RNA (SSU rRNA) gene sequences and molecular phylogenetic analyses using these sequences show

that there are several unidentified lineages around or within the cryptomonads (Kim and Archibald 2013; Shalchian-Tabrizi et al. 2008). These lineages are potentially significant for revealing the evolution and process of acquiring plastids and for filling the morphological and ultrastructural gap between cryptomonads and katablepharids.

In this study, we report a novel heterotrophic cryptomonad that was collected from a seaweed sample in the Republic of Palau. We conducted light and electron microscopic observations, as well as a molecular phylogenetic analyses of the new cryptomonad, using small and large subunit ribosomal RNA genes. These investigations revealed the morphology, ultrastructure, and phylogenetic position of the new cryptomonad and provided significant information for discussing the diversity and evolution of cryptomonads.

MATERIALS AND METHODS

Sample collection and culture establishment

A sample of seaweed (*Padina* sp.) was collected north of Mecherchar Island, Koror, Republic of Palau (latitude = 7.1564 °N, longitude = 134.3590 °E) on November 4, 2011. The seaweed was washed with seawater that was collected at the same location, and several drops of the wash were added to ESM medium (Kasai et al. 2009) and kept at 20 °C, under a 14-h light/10-h dark cycle. A clonal culture of *Hemiarma marina* n. g., n. sp. (strain SRT149) was then established from the enriched sample by single-cell isolation using a micropipette. The strain was maintained in ESM medium at 20 °C, under dark conditions, and with contaminant bacteria as a food source.

Light and electron microscopic observation

Living cells of *H. marina* were observed on microscope slides using a Zeiss Axio imager A2 microscope (Zeiss, Oberkochen, Germany) equipped with an Olympus DP71 CCD

camera (Olympus, Tokyo, Japan) or on a glass bottom Petri dish using an Olympus IX71 inverted microscope (Olympus, Tokyo, Japan) equipped with an Olympus DP73 CCD camera (Olympus, Tokyo, Japan).

For scanning electron microscopy (SEM), specimens were prepared with chemical and freeze substitution fixation. The chemical fixation was performed as follow; cells in culture media were mounted onto 8.5-mm diameter glass SEM plates (Okenshoji Co., Tokyo, Japan) that were coated with 0.1% (w/v) poly-L-lysine (Sigma Chemical Co., St. Louis, MO). Cells were prefixed with OsO_4 vapor for 30 min at room temperature and subsequently postfixed with 1% (w/v) OsO_4 for 1h at room temperature. The fixed cells on the glass plate were gradually dehydrated using an ethanol series of 15-100% ethanol. After dehydration, the specimen was placed in a 1:1 mixture of 100% ethanol and 100% *t*-butyl alcohol, which was subsequently replaced with 100% *t*-butyl alcohol. The specimen in 100% *t*-butyl alcohol was then frozen in a freezer and freeze-dried using a VFD-21S freeze-drier (SHINKU-DEVICE, Ibaraki, Japan). The freeze substitution fixation was performed as follow; cells were collected by centrifugation (2500 *g* for 7 min). The cell pellets were placed on a Formvar-coated copper loop and plunged rapidly into liquid propane. The frozen pellets were then plunged into liquid nitrogen for several seconds and placed in 2% (w/v) osmium tetroxide in acetone at -80 °C for 48 h, -20 °C for 2 h, and 4 °C for 2 h. The pellets were rinsed three times with acetone. The cell pellets were placed in a 1:1 mixture of 100% ethanol and 100% *t*-butyl alcohol which was subsequently replaced with 100% *t*-butyl alcohol. The cell pellets were resuspended by pipetting and mounted on 8.5-mm diameter glass SEM plates (Okenshoji Co., Tokyo, Japan) that were coated with 0.1% (w/v) poly-L-lysine (Sigma Chemical Co., St. Louis, MO) or 0.4 μm pore size Isopore membrane filter (Millipore Corporation, Billerica, MA, USA). The specimen in 100% *t*-butyl alcohol was then frozen in a freezer and freeze-dried using a VFD-21S

freeze-drier (SHINKU-DEVICE, Ibaraki, Japan). The mounted specimens were coated with platinum-palladium using a Hitachi E1045 (Hitachi High-Technologies Corp., Tokyo, Japan) and then observed under a JSM-6360F field emission SEM (JEOL, Tokyo, Japan).

For transmission electron microscopy, cells were collected by centrifugation (2500 *g* for 7 min). The cell pellets were placed on a Formvar-coated copper loop and plunged rapidly into liquid propane. The frozen pellets were then plunged into liquid nitrogen for several seconds and placed in 2% (w/v) osmium tetroxide in acetone at -80 °C for 48 h, -20 °C for 2 h, and 4 °C for 2 h. The pellets were rinsed three times with acetone and replaced by Agar Low Viscosity Resin R1078 (Agar Scientific Ltd, Stansted, England), which was polymerized by heating at 60 °C for 12 h. For the observation of periplasts (Figure 4), we prepared a TEM specimen by chemical fixation; cells were collected by centrifugation and subsequently pre-fixed using a mixture of 2% (w/v) glutaraldehyde, 0.25 M sucrose, and 0.1 M sodium cacodylate buffer (pH 7.2, SCB) for 1 h at room temperature. Fixed cells were washed three times with 0.2 M SCB and then post-fixed using 1% (w/v) OsO_4 with 0.1 M SCB for 30 min at 4 °C. Cells were dehydrated in a graded ethanol series beginning at 30% and ending at 100% (v/v). After dehydration, cells were placed in 1:1 mixture of 100% ethanol and acetone for 10 min, followed by two 10 min intervals in acetone. Resin replacement was performed using a 1:1 mixture of acetone and Agar Low Viscosity Resin R1078 (Agar Scientific Ltd., Stansted, England) for 30 min, followed by pure resin for 2 h. Resin was polymerized by heating at 60 °C for 12 h. Ultrathin sections of each specimen was prepared on a Reichert Ultracut S ultramicrotome (Leica, Vienna, Austria), double stained with 2% (w/v) uranyl acetate and lead citrate (Hanaichi et al. 1986; Sato 1968), and observed using a Hitachi H-7650 electron microscope (Hitachi High-Technologies Corp., Tokyo, Japan) equipped with a Veleta TEM CCD camera (Olympus Soft Imaging System, Munster, Germany).

DNA extraction, amplification, and sequencing

Total DNA of *H. marina* was extracted from centrifuged cells pellets using the DNeasy Plant mini kit (Qiagen, Hilden, Germany). Polymerase chain reaction (PCR) was performed on the total DNA using SR1-SR12 primers (Nakayama et al. 1998) for the small subunit ribosomal RNA (SSU rRNA) gene and L1-L12 primers (Yabuki et al. 2010) for the large subunit ribosomal RNA (LSU rRNA) gene. Amplifications consisted of 30 cycles of denaturation at 94 °C for 30 s, annealing at 55 °C for 30 min, and extension at 72 °C for 2-4 min, depending on the expected size of PCR fragments. Amplified DNA fragments were purified after gel electrophoreses with a QIAquick Gel Extraction Kit (Qiagen, Hilden, Germany) and then cloned into the p-GEM® T-easy vector (Promega, Tokyo, Japan). The inserted DNA fragments were completely sequenced with a 3130 Genetic Analyzer (Applied Biosystems, CA, USA), using the BigDye Terminator v3.1 cycle sequencing kit (Applied Biosystems, CA, USA). The SSU and LSU rRNA gene sequences of the strain SRT149 were deposited as LC151286 and LC151287 in GenBank, respectively.

Sequence alignments and phylogenetic analysis

We newly created alignment sets for molecular phylogenetic analyses of SSU rRNA gene and concatenated SSU and LSU rRNA gene. SSU and LSU rRNA gene sequences of the strain SRT149 were added to these alignment sets, respectively. The alignment sets were automatically aligned with MAFFT (Katoh and Toh 2008) and then edited manually with SeaView (Galtier et al. 1996). Ambiguously aligned regions were manually deleted from each alignment. These alignment files are available on request.

Model selection for molecular phylogenetic analyses was performed using Kakusan4 (Tanabe 2007) and GTR+Γ model was selected as the best-fit model. For each alignment, the maximum likelihood (ML) tree was heuristically searched using RAxML v.8.0.3 (Stamatakis 2014) under the GTR+Γ model. Tree searches started with 20

randomized maximum-parsimony trees, and the highest log likelihood (lnL) was selected as the ML tree. An ML bootstrap analysis (1,000 replicates) was conducted under the GTR+Γ model with the rapid bootstrap option. A Bayesian analysis was run using MrBayes v. 3.2.2 (Ronquist and Huelsenbeck 2003) with the GTR +Γ model for each dataset. One cold and three heated Markov chain Monte Carlo chains with default temperatures were run for 5×10^6 generations, sampling lnL values and trees at 100-generation intervals. The first 25% (1.25×10^6) of generations in each analysis was discarded as "burn-in," and Bayesian posterior probabilities (BPP) and branch lengths were calculated from the remaining trees.

RESULTS

Light microscopy

Cells were subspherical or ovoid, slightly dorsoventrally flattened, and 3.9 μm (2.9–5.4 μm, n = 80) in length (Fig. 1). Two flagella emerged from the right anterior part of the cell and were arranged dorsoventrally (Fig. 1A–E). Two rows of ejectisomes were located on the anterior surface of the cell (Fig. 1A, D, F), and each row consisted of 3–5 ejectisomes that were arranged approximately in parallel (Fig. 1F). Dividing cells also had the two rows of ejectisomes on the anterior surface of the cell (Fig 1G–J). Cells containing large food vacuoles were occasionally observed (Fig. 1A, D). In the growth phase, most of the cells attached to the substrate using their posterior flagella (Fig. 1A–C), and the attached cells displayed a jumping motion (Movie S1). Cells were occasionally detached from the substrate and then swam in the water column. The number of swimming cells increased as the culture aged. The cells swam forward with a rapid rotating movement, or rotated in place like a spinning top (Movie S2).

Scanning electron microscopy

The right side of the cell surface was tightly covered by irregular polygonal periplast plates,

whereas the left half of the cell surface was naked (Fig. 2A–E). The periplast plates varied in size and shape (Fig. 2A–C), and the total number of plates varied among individuals. Two unequal flagella were arranged in parallel and emerged from right anterior part of the cell (Fig. 2A, D, E). The anterior flagellum was slightly longer than posterior flagellum and possessed fibrillar hairs without base and terminal filament (Fig. 2A, G); the posterior flagellum was naked (Fig. 2A). In some individuals, a depression was observed at the left side of the flagellar insertion point (Fig. 2F).

Transmission electron microscopy

The cells possessed a nucleus that contained permanently condensed chromatin and a conspicuous nucleolus (Fig 3A–C) and that was located in the ventral region (Fig. 3B, C). A Golgi apparatus was situated near the right anterior side of the nucleus (Fig. 3A, B). A large mitochondrion with flat cristae was located in dorsal region (Fig. 3B), and a well-developed rough endoplasmic reticulum was closely associated to the mitochondrion (Fig. 3B, C). Large food vacuoles were occasionally observed in the posterior or left region of cells (Fig. 3B). Thin periplast plates that covered the outer surface of plasma membrane were also observed (Fig. 3D, 4). The periplast plates were well recognized in the chemical fixation specimen than the freeze substitution fixation specimen. The difference was probably caused by the cell shrinking by chemical fixation and low contrast of membrane structures in freeze substitution fixation. The periplast plates were less dense than cell membrane, and not observed at left side of the cell (Fig. 4A, B) and gaps between periplast plates (Fig. 4C). The two rows of large (type1) ejectisomes were located just beneath the anterior plasma membrane (Fig. 5A), and each ejectisome contained two coiled ribbon structures (Fig. 5B). Small (type2) ejectisomes also contained two coiled ribbon structures and were scattered just beneath of the cell surface (Fig. 5C). In addition, some individuals had an anterior depression at the dorsal side of the flagellar insertion point (Fig. 5D). A microtubular band

and small electron dense vesicles lined the ventral side of the depression (Fig. 5D). The transitional region of the basal body included a septum, the center of which was depressed and encloses the axosome (Fig. 6A, B). Thin nonagonal fibers were also observed in the transitional region, proximal to the septum (Fig. 6D).

Molecular phylogeny

In our phylogenetic analysis using the SSU rRNA gene, *H. marina* formed a clade with two marine environmental sequences (FJ537320, GU824726) (Fig. 6). The clade of *H. marina* and the two environmental sequences placed as a sister lineage of the freshwater environmental clade, which has been recognized as CRY1 (Shalchian-Tabrizi et al. 2008), with high statistical supports. Here, we refer to the freshwater environmental sequence clade as CRY1a and the marine environmental sequence clade, including *H. marina,* as CRY1b. In the SSU rRNA gene tree, both CRY1a and b were placed at the base of the Cryptomonada clade with weak statistical support. In addition, the monophyly of the Cryptomonada and the CRY1a and b clades was not strongly supported, with a bootstrap probability (BP) of 56% and a Bayesian posterior probability (BPP) of 0.8465. However, in the concatenated SSU and LSU rRNA gene tree, the monophyly of *Goniomonas* was robustly supported (BP = 100%, BPP = 1), and *H. marina* formed a moderately supported clade with *Goniomonas* (BP = 71%, BPP = 0.9674) (Fig. 7).

DISCUSSION

Taxonomic position of *Hemiarma marina* n. g., n. sp.

In this study, we reported a novel heterotrophic cryptomonad, *H. marina* from a seaweed sample from the Republic of Palau. Our phylogenetic analyses showed that *H. marina* was placed in the cryptomonad environmental clade CRY1b. Light and electron microscopic observations also showed that *H. marina* shares ultrastructural features with other

cryptomonads, such as ejectisomes that consist of two coiled ribbon structures, mitochondria with flat cristae, and a periplast cell covering. Here, we perform a detailed morphological and ultrastructural comparison between *H. marina* and other cryptomonads, in order to reveal its taxonomic position.

The cell behavior of *H. marina* is quite different from that of other cryptomonads. Cryptophyceans usually swim in the water column while rotating around their longitudinal axis (Gillott 1990), and *Goniomonas* swims on the surface of substrates with 'waggling' or 'jerky' movements or swims in the water column while rotating around its longitudinal axis (Hill 1991; Kim and Archibald 2013). The cells of *H. marina* also exhibit a rotating motion when swimming, but it differs from other cryptomonads by rapidly rotating in place, like a spinning top. Furthermore, in growth phase cultures, most of the *H. marina* cells attach to the substrate using their posterior flagella and display a jumping motion. Although some phagotrophic stramenopiles (*Halocafeteria seosinensis*) and Englenozoa (*Bodo saltans*) exhibit similar behaviors, these have not been reported in cryptomonads (Park et al. 2006; Patterson and Simpson 1996).

H. marina is more similar to *Goniomonas* than to the photosynthetic cryptomonads in having large ejectisomes that are arranged transversely at the anterior region of the cell (Kim and Archibald 2013; Kugrens and Lee 1991; Martin-Cereceda et al. 2010). Since the large ejectisomes of cryptophyceans and katablepharids are arranged longitudinally, the similar arrangement of large ejectisomes among *H. marina* and *Goniomonas* may suggest relatedness (e.g. Clay and Kugrens 1999; Okamoto and Inouye 2006; Okamoto et al. 2009; Vørs 1992).

All cryptomonads possess a longitudinal groove (furrow) and/or invagination (gullet) (Kugrens and Lee 1991; Kugrens et al. 2002), and *Goniomonas* possesses an additional opening (infundibulum) that is presumably used for the ingestion of food

organisms (Kugrens and Lee 1991; Kugrens et al. 2002). Although we could not recognize a furrow-gullet complex in *H. marina*, a depression was observed at the dorsal anterior region of some cells. The depression probably corresponds with the infundibulum of *Goniomonas* because of the positional similarity and the existence of electron-dense vesicles that are also known to border a side of the infundibulum (Kim and Archibald 2013; Kugrens and Lee 1991). On the other hand, the depression was not observed in all the cells, which suggests that it could be a temporal structure that is only open when the cells are feeding.

The periplast is a specific cell covering of cryptomonads that consists of a plasma membrane and inner and outer components (Clay et al. 1999; Kugrens et al. 2002). The periplasts of cryptomonads cover the entire cell surface but do not extend into the vestibulum or the gullet/furrow region (Gillott 1980). The shape and arrangement of periplast plates also show variation and can be used as taxonomic traits (Clay et al. 1999; Gillott 1980). The periplast of *H. marina* is similar to that of *Goniomonas* in consisting of a relatively small number of the plates (Kim and Archibald 2013; Martin-Cereceda et al. 2010); however, the periplast of *H. marina* consists of irregular polygonal plates that are different from the rectangular plates of *Goniomonas*. Moreover, *H. marina* does not possess a furrow-gullet complex or vestibulum, and the left half of the cell surface lacks periplast plates. It is not clear whether the naked region of the cell surface, which is larger than in other cryptomonads, is the trace of an ancestral cryptomonad or of a secondary reduction of the periplast plates.

In cryptomonads, various types of flagellar appendages are reported (e.g. hairs, scales, and spines). Members of the Cryptophyceae possess bipartite tubular hairs on at least one flagellum (Kugrens et al. 1987), and flagellar scales with seven-sided rosette patterns are reported in some photosynthetic cryptophyceans (Lee and Kugrens 1986).

Alternatively, *Goniomonas* possesses fibrillar hairs on the at least anterior flagellum (Kim and Archibald 2013; Kugrens and Lee 1991; Martin-Cereceda et al. 2010), and only the freshwater species *G. truncata* possesses fibrillar hairs on both flagella and curved spikes on one flagellum (Kugrens and Lee 1991). *H. marina* possesses fibrillar hairs on its anterior flagellum and neither scales nor spines were observed, which again suggests that *H. marina* is more closely related to *Goniomonas* than to other cryptophyceans.

The flagellar transitional region of cryptomonads has two or more plate-like partitions, and the central pair of axosomes terminates at the uppermost partition (Graham et al. 2009; Grain et al. 1988; Moestrup 1982). The transitional region of *H. marina* is different from that of other cryptomonads in possessing only one septum. Since transitional regions with one plate-like partition are reported in another cryptist assemblage, the Katablepharids, the transitional region of *H. marina* may retain an ancestral trait (Lee et al. 1992). However, a depressed septum that encloses the axosome, as seen in *H. marina*, has not been reported. *H. marina* also possesses nonagonal fibers at the proximal side of the depressed septum. The nonagonal fibers have not been reported in Cryptista but are common in Cercozoan flagellates (Cavalier-Smith et al. 2008). However, it is unclear whether the nonagonal fibers of *H. marina* are homologous with those of cercozoans, since cercozoan nonagonal fibers are located distal to the transitional region.

As a whole, the above-mentioned morphological and ultrastructural comparisons and molecular phylogenetic analyses provide evidence that *H. marina* is a novel cryptomonad and different from known taxonomic groups. As such, we treat *H. marina* as new genus and species of cryptomonad. *H. marina* shares several morphological and ultrastructural characteristics with *Goniomonas*, which corresponds with the tree topology of combined SSU and LSU rRNA genes.

H. marina and environmental sequences around Cryptomonada

Marine-freshwater transitions are considered to be uncommon in cryptomonads (Shalchian-Tabrizi et al. 2008). Our molecular phylogenetic analysis using 18S rRNA gene revealed a novel clade (CRY1b) that consists of *H. marina* and two environmental sequences (GU824726 and FJ537320). These three sequences of the CRY1b clade are derived from marine samples/organisms and form a clade with the freshwater environmental clade CRY1a, which indicates a new example of marine-freshwater transition in cryptomonads.

Despite the fact that all described cryptomonads are aerobic, one environmental sequence of CRY1b (GU824726) was obtained from a micro-oxic water column (Edgcomb et al. 2011). Edgcomb et al. (2011) also discovered a marine environmental sequence that belonged to the CRY3 clade from a micro-oxic water column (GU823791), which suggests the possibility of low-oxygen adaptation by basal cryptomonads, although it is unclear that these sequences were extracted from cells that grow in the micro-oxic environment.

The three sequences of the CRY1b (GU824726, FJ537320, and *H. marina*) are divergent from one another, and the recently obtained CRY3 sequence (GU823791) is also distant from the other CRY3 sequences. These sequences may represent undescribed genera or species of cryptomonads, respectively. Thus, it is necessary to perform taxonomic studies on these undescribed lineages, in order to understand the diversity and evolution of the cryptomonads.

TAXONOMIC SUMMARY

Cryptista; Cryptomonada

***Hemiarma* n. gen.**

Diagnosis. Heterotrophic biflagellate. Two flagella emerging from right anterior side of the cell in parallel and arranged dorsoventrally. Periplast plates covering right half region of

cell surface. Two rows of ejectisomes arranged laterally at anterior region of the cell. Transitional region with nonagonal fiber and single septum, the middle of which is depressed.

Type species. *Hemiarma marina*

Etymology. The genus name "*Hemiarma*" is derived from the Greek *Hemi* (half) and *arma* (defensive armor), which refers to the periplast plates that cover only the right half region of cell surface. *Hemiarma* is neuter.

***Hemiarma marina* n. sp.**

Diagnosis. Cells subspherical or ovoid, about 3.9 μm (2.9–5.4 μm) in length. Cells attaching to the substrate using the posterior flagellum and displaying a jumping motion, or swimming in the water column with rotating motion. Periplast of irregular polygonal plates. The anterior flagellum slightly longer than the posterior flagellum and with fibrillar hairs.

Hapantotype. One microscope slide (TNS-AL-58927a), deposited in the herbarium of the National Museum of Nature and Science (TNS), Tokyo.

Paratype. One EM block (TNS-AL-58927b) at TNS. These cells are derived from the same sample as the hapantotype.

DNA sequence. SSU rRNA gene, LC151286. LSU rRNA gene, LC151287.

Type locality. A seaweed (*Padina* sp.) collected north of Mecherchar Island, Koror, Palau (latitude = 7.1564 °N, longitude = 134.3590 °E).

Collection date. November 4, 2011.

Type strain. The strain used for describing the hapantotype is maintained at the National Institute for Environmental Studies (NIES, Tsukuba, Japan) as NIES-3956.

Etymology. The specific epithet "*marina*" (marine) refers to the habitat of the species.

ACKNOWLEDGEMENTS

Acknowledgements

We thank the Ministry of Natural Resources, Environment, and Tourism, Palau, for providing permits for collecting marine resources (permit number, RE-11-18). We thank Dr. Naoto Hanzawa at Yamagata University for trip management for sampling. This work was supported by JSPS KAKENHI Grant Numbers 13J00587 and 23405013.

LITERATURE CITED

Archibald, J.M., & Keeling, P.J. 2002. Recycled plastids: a green movement in eukaryotic evolution. *Trends Genet.,* 18:577-584.

Clay, B.L. & Kugrens, P. 1999. Systematics of the enigmatic Kathablepharids, including EM characterization of the type species, *Kathablepharis phoenikoston*, and new observations on *K. remigera* comb. nov. *Protist,* 150:43-59.

Clay, B. L., Kugrens, P. & Lee, R. E. 1999. A revised classification of Cryptophyta. *Bot. J. Linn. Soc*., 131:131-151.

Edgcomb, V., Orsi, W., Bunge, J., Jeon, S., Christen, R., Leslin, C., Holder, M., Taylor, G.T., Suarez, P., Varela, R. & Epstein, S. 2011. Protistan microbial observatory in the Cariaco Basin, Caribbean. I. Pyrosequencing vs Sanger insights into species richness. *Int. Soc. Microb. Ecol. J.,* 5:1344-1356.

Galtier, N., Gouy, M. & Gautier, C. 1996. SEAVIEW and PHYLO_WIN: two graphic tools for sequence alignment and molecular phylogeny. *Comput. Appl. Biosci.,* 12:543-548.

Gillott, M. 1990. Phylum Cryptophyta (Cryptomonads). *In:* Handbook of Protoctista. Margulis, L., Corliss, J., Melkonian, M. & Chapman, D.J. (ed.), Jones and Bartlett, Boston, Massachusetts. p. 148-151.

Graham, L.E., Graham, J.M. & Wilcox, L.W. 2009. Algae. Benjamin Cummings (Pearson),

San Francisco, California. p. 159-169

Grain, J., Mignot, J.-P. & Putorac, P. 1988. Ultrastructures and evolutionary modalities of flagellar and ciliary systems in protists. *Biol. Cell,* 63:219-237.

Hanaichi, T., Sato, T., Hoshino, M. & Mizuno, N. 1986. A stable lead stain by modification of Sato's method. Proceedings of the XIth International Congress on Electron Microscopy, Japanese Society for Electron Microscopy, Kyoto, Japan, pp. 2181–2182.

Heywood, P. 1988. Ultrastructure of *Chilomonas paramecium* and the phylogeny of the cryptoprotists. *BioSystems*, 21:293-298.

Hill, D. R. A. 1991. Diversity of heterotrophic cryptomonads. *In:* Patterson, D. J. & Larsen, J. (ed.), The Biology of Free-Living Heterotrophic Flagellates. Clarendon Press, Oxford, England. p. 235–240.

Kasai, F., Kawachi, M., Erata, M., Mori, F., Yumoto, K., Sato, M. & Ishimoto, M. 2009. NIES-Collection, List of strains, 8th edition. *Jpn. J. Phycol. (Sôrui),* 57:1-350.

Katoh, K. & Toh, H. 2008. Recent developments in the MAFFT multiple sequence alignment program. *Brief. Bioinform.,* 9:286-298.

Kim, E. & Archibald, J.M. 2013. Ultrastructure and molecular phylogeny of the cryptomonad *Goniomonas avonlea* sp. nov. *Protist*, 164:160-182.

Kugrens, P., Lee, R.E. & Andersen, R.E. 1987. Ultrastructural variations in cryptomonad flagella. *J. Phycol.,* 23:511-18.

Kugrens, P. & Lee, R. E. 1991. Organization of cryptomonads. *In:* Patterson, D.J. & Larsen, J. (ed.), The Biology of Free-living Heterotrophic Flagellates. Clarendon Press, Oxford. p. 219-233.

Kugrens, P., Lee, R. E. & Hill, D. R. A. 2002. Order Cryptomonadida. *In:* Lee, J. J., Leedale, G. F. & Bradbury, P. (ed.), An Illustrated Guide to the Protozoa. 2nd ed. Society of Protozoologists, Lawrence, KS. p. 1111-1125.

Lee, R.E. & Kugrens, P. 1986. The occurrence and structure of flagellar scales in some freshwater cryptophytes. *J. Phycol.,* 22:549-52.

Lee, R.E., Kugrens, P. & Mylnikov, A.P. 1992. The structure of the flagellar apparatus of two strains of *Katablepharis* (Cryptophyceae). *Brit. Phycol. J.,* 27:369-380.

Martin-Cereceda, M., Roberts, E.C., Wootton, E.C., Bonaccorso, E., Dyal, P., Guinea, A., Rogers, D., Wright, C.J. & Novarino, G. 2010. Morphology, ultrastructure, and small subunit rDNA phylogeny of the marine heterotrophic flagellate *Goniomonas* aff. *amphinema*. *J. Eukaryot. Microbiol*., 57:159-170.

Moestrup, Ø. 1982. Flagellar structure in algae: a review with new observations particularly on the Chrysophyceae, Phaeophyceae (Fucophyceae), Euglenophyceae, and *Reckertia*. *Phycologia*, 21:427-528.

Nakayama, T., Marin, B., Kranz, H.D., Surek, B., Huss, V.A.R., Inouye, I. & Melkonian, M. 1998. The basal position of scaly green flagellates among the green algae (Chlorophyta) is revealed by analyses of nuclear-encoded SSU rRNA sequences. *Protist,* 149:367-380.

Okamoto, N., Chantangsi, C., Horàk, A., Leander, B.S., Keeling & P.J. 2009. Molecular phylogeny and description of the novel katablepharid *Roombia truncata* gen. et sp. nov., and establishment of Hacrobia taxon nov. *PLoS ONE*, 4, e7080.

Okamoto, N. & Inouye, I. 2005. The katablepharids are a distant sister group of the Cryptophyta: a proposal for Katablepharidophyta divisio nova/Kathablepharida phylum novum based on SSU rDNA and beta-tubulin phylogeny. *Protist,* 156:163-179.

Okamoto, N. & Inouye, I. 2006. *Hatena arenicola* gen. et sp. nov., a katablepharid undergoing probable plastid acquisition. *Protist,* 157:401-419.

Park, J.S., Cho, B.C. & Simpson, A.G.B. 2006. *Halocafeteria seosinensis* gen. et sp. nov. (Bicosoecida), a halophilic bacterivorous nanoflagellate isolated from a solar saltern.

Extremophiles, 10:493-504.

Patterson, D.J. & Simpson, A.G.B. 1996. Heterotrophic flagellates from coastal marine and hypersaline sediments in Western Australia. *Eur. J. Protistol.,* 32:423-448.

Ronquist, F. & Huelsenbeck, J. P. 2003. MrBayes 3: bayesian phylogenetic inference under mixed models. *Bioinformatics*, 19:1572-1574.

Sato, T. 1968. A modified method for lead staining of thin sections. *J. Electron Microsc.,* 17:158-159.

Sepsenwol, S. 1973. Leucoplast of the cryptomonad *Chilomonas paramecium*; evidence for the presence of a true plastid in a colourless flagellate. *Exp. Cell Res.,* 76:395-409.

Shalchian-Tabrizi, K., Bråte, J., Logares, R., Klaveness, D., Berney, C. & Jakobsen, K. 2008. Diversification in unicellular eukaryotes: cryptomonad colonizations of marine and freshwaters inferred from revised 18S rRNA phylogeny. *Environ. Microbiol.,* 10:2635-2644.

Stamatakis, A. 2014. RAxML version 8: A tool for phylogenetic analysis and post-analysis of large phylogenies. *Bioinformatics*, 30:1312-1313.

Tanabe AS. (2011). Kakusan4 and Aminosan: two programs for comparing nonpartitioned, proportional and separate models for combined molecular phylogenetic analyses of multilocus sequence data. *Mol*. *Ecol*. *Resour*., 11:914-921.

Vørs, N. 1992. Ultrastructure and autecology of the marine heterotrophic flagellate *Leucocryptos marina* (Braarud) Butcher 1967 (Katablepharidaceae/Kathablepharidae), with a discussion of the genera *Leucocryptos* and *Katablepharis*/*Kathablepharis*. *Eur. J. Protistol.,* 28:369-389.

Yabuki, A., Inagaki, Y. & Ishida, K. 2010. *Palpitomonas bilix* gen. et sp. nov.: a novel deep-branching heterotroph possibly related to Archaeplastida or Hacrobia. *Protist*, 161:523-538.

FIGURE LEGEND

Fig. 1. Light micrographs of *Hemiarma marina* n. g., n. sp. **A–C**, **E–F**, and **H–J** picture three individual cells. **A–C.** Dorsal view of an attached cell, focusing from dorsal to ventral. **D**. Dorsal view. **E–F.** Anterior view. **G–J.** Dividing cells. AF, anterior flagellum; FV, food vacuole; PF, posterior flagellum; Arrowheads indicate large ejectisomes. Scale bar = 5 μm.

Fig. 2. Scanning electron micrograph of *Hemiarma marina* n. g., n. sp. Cells in **A, B, D, G** were fixed by chemical fixation. Cells in **C, F, F** were fixed by freeze substitution fixation. **A.** Dorsal view. **B, C.** Right view. **D, E.** Anterior view. **F.** Anterior view, showing anterior depression. **G.** High magnification view of anterior flagellum. AF, anterior flagellum; PF, posterior flagellum. White arrow indicates an anterior depression. White arrowheads indicate fibrillar hairs. White double arrowheads indicate periplast plates. Scale bars = 1 μm.

Fig. 3. Transmission electron micrograph of *Hemiarma marina* n. g., n. sp. by freeze substitution fixation. **A.** Approximately longitudinal section. Scale bar = 1 μm. **B, C.** Approximately transverse section. Scale bar = 500 nm. **D.** High magnification view of cell surface. Scale bar = 200 nm. **E.** High magnification view of a gap between periplast plates. Scale bar = 200 nm. AB, anterior basal body; ER, endoplasmic reticulum; F, flagellum; G, Golgi apparatus; M, mitochondrion; N, nucleus; n, nucleolus; PB, posterior basal body. Double arrows indicate periplast plate. Arrowheads indicate large ejectisomes.

Fig. 4. Transmission electron micrograph of *Hemiarma marina* n. g., n. sp. by chemical fixation. A. Whole cell image showing periplast plates. Scale bar = 1 μm. B. High

magnification view of gap between periplast plates. Scale bar = 200 nm. C. High magnification view of the boundary of periplast plate (left) and naked region (right). Scale bar = 200 nm. M, mitochondrion; N, nucleus; n, nucleolus. Double arrows indicate periplast plate. Wide arrowhead indicates gap between the periplast plates.

Fig. 5. Transmission electron micrograph of *Hemiarma marina* n. g., n. sp. by freeze substitution fixation. **A.** Approximately transverse section of anterior region, showing the two rows of ejectisomes. Scale bar = 1 μm. **B.** High magnification view of a large ejectisome. Scale bar = 200 nm. **C.** High magnification view of a small ejectisome. Scale bar = 200 nm. **D.** Approximately transverse section of anterior region, showing the anterior depression. Scale bar = 1 μm. AF, anterior flagellum; D, anterior depression; N, nucleus; PB, posterior basal body; Arrows indicate electron dense vesicles. Arrowheads indicate large ejectisomes. Double arrowheads indicate coiled ribbon structure in large ejectisome. Triple arrowheads indicate coiled ribbon structure in small ejectisome.

Fig. 6. Transmission electron micrograph of *Hemiarma marina* n. g., n. sp. by freeze substitution fixation. **A.** Longitudinal section of the flagellum, transitional region, and basal body. B–D correspond with approximate position of Fig 5B–D, respectively. **B–D.** Serial transverse sections of flagellum and transitional region. S, septum, the center of which is depressed; NF, nonagonal fiber. Scale bars = 200 nm.

Fig. 7. Maximum-likelihood tree of Cryptomonada using 1,652 positions of the small subunit ribosomal RNA gene. Environmental sequences were labeled with accession numbers. Only bootstrap probabilities ≥ 50% are shown. Nodes that are supported by Bayesian posterior probabilities ≥ 0.95 are indicated by bold lines.

Fig. 8. Maximum-likelihood tree of Cryptomonada using 1,650 positions of the small subunit ribosomal RNA gene and 2,763 positions of the large subunit ribosomal RNA gene. Dashed branch is shortened to half of its original length. Only bootstrap probabilities ≥ 50% are shown. Nodes that are supported by Bayesian posterior probabilities ≥ 0.95 are indicated by bold lines.

SUPPORTING INFORMATION

Movie S1. Attached cell of *Hemiarma* marina n. g., n. sp., showing jumping motion.

Movie S2. Spinning cell of *Hemiarma* marina n. g., n. sp.

Fig. 1

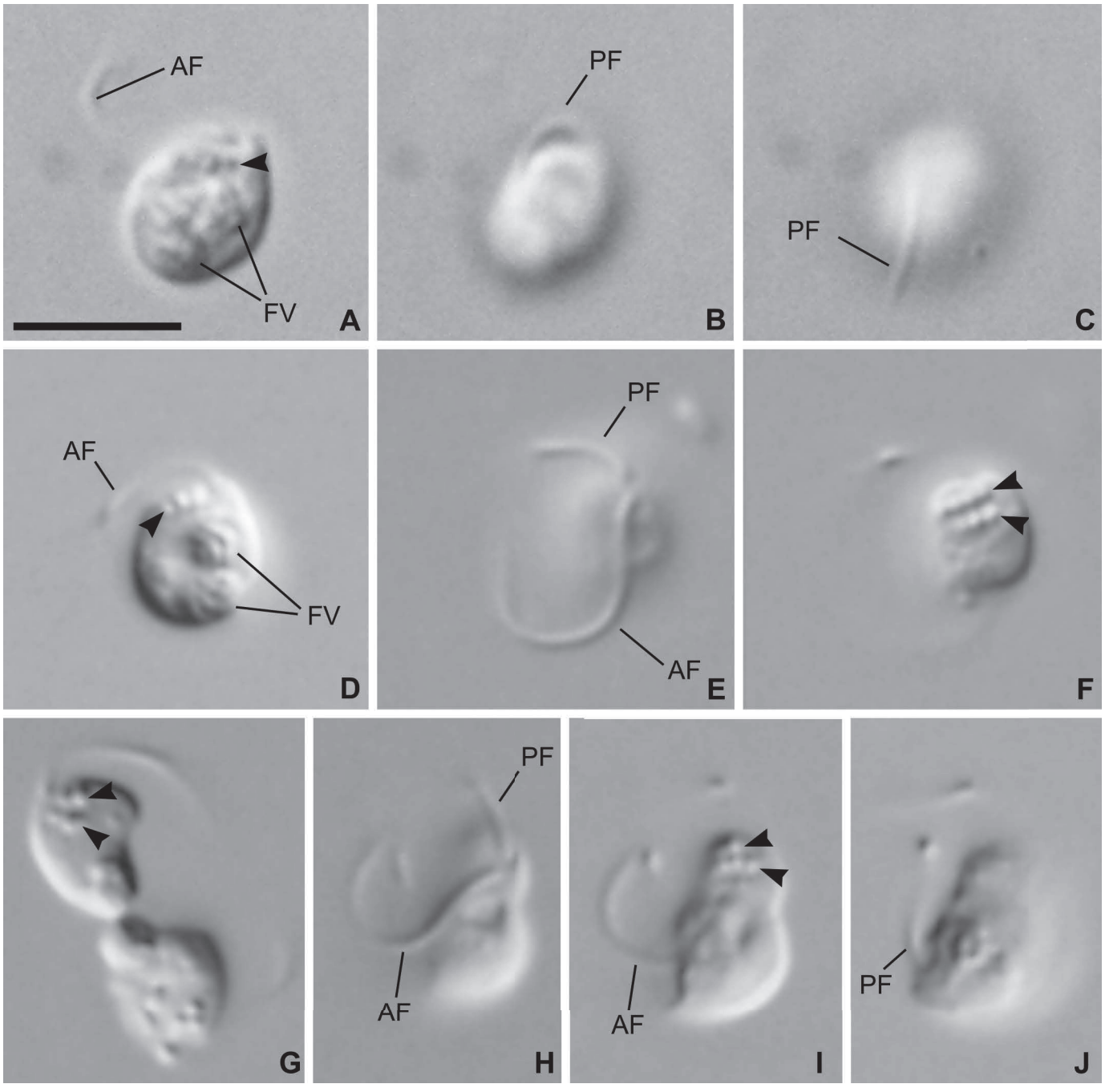

Fig. 2

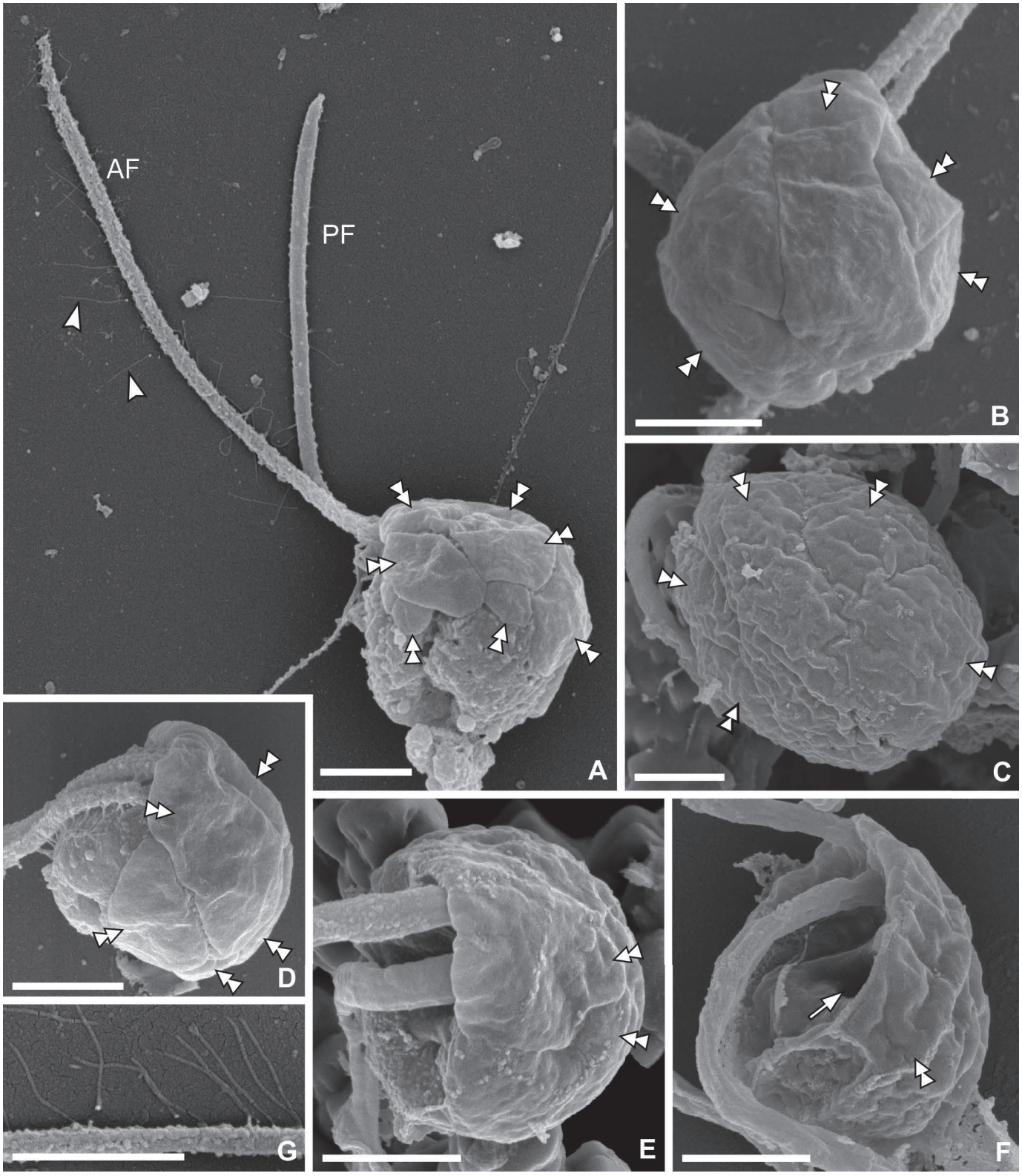

Fig. 3

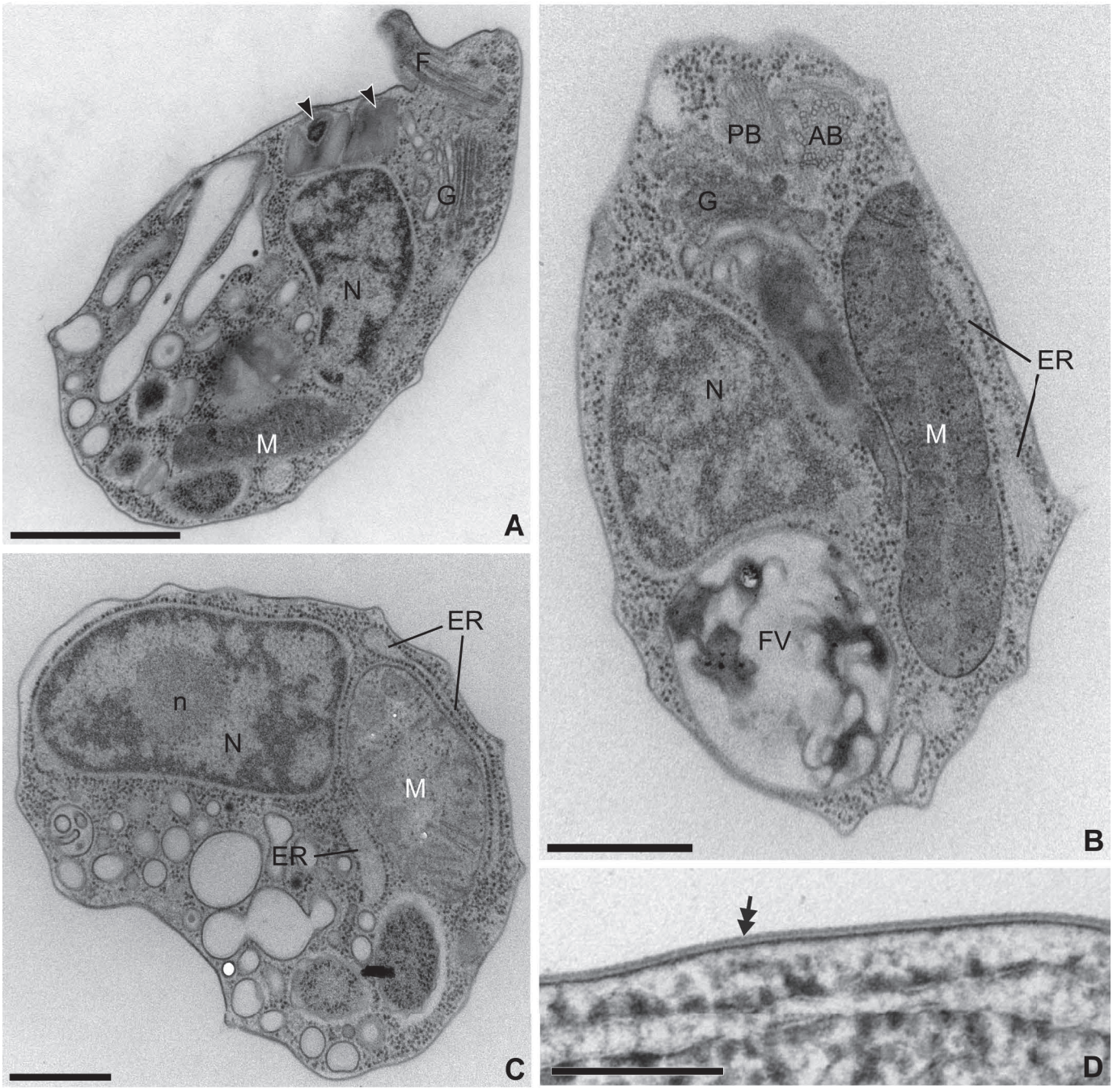

Fig. 4

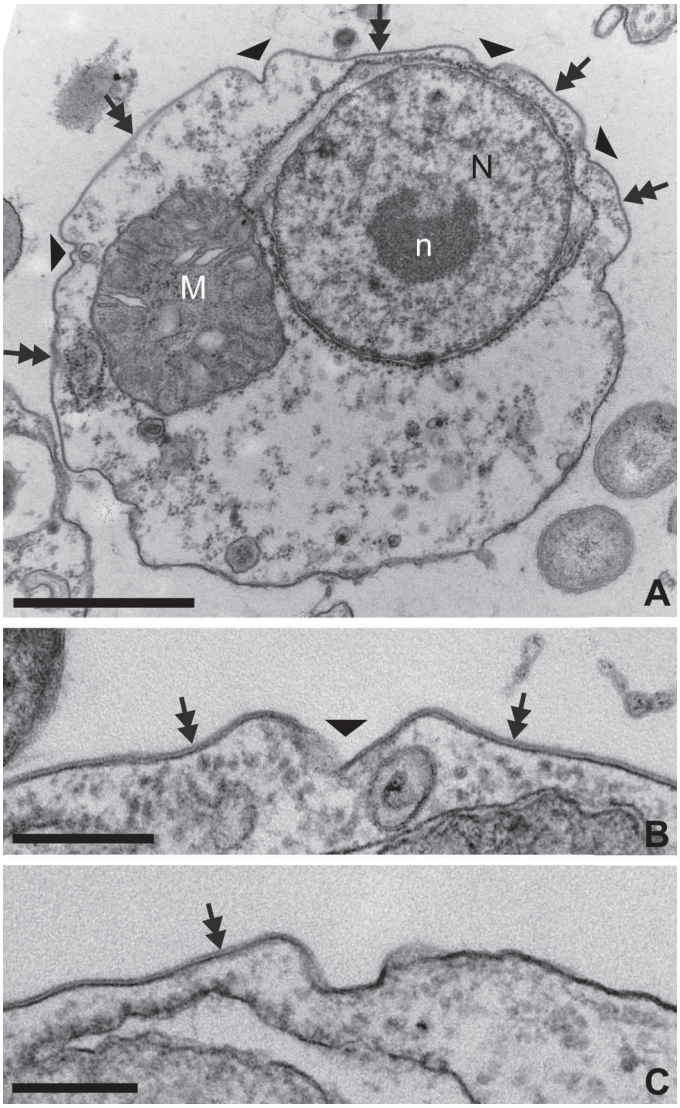

Fig. 5

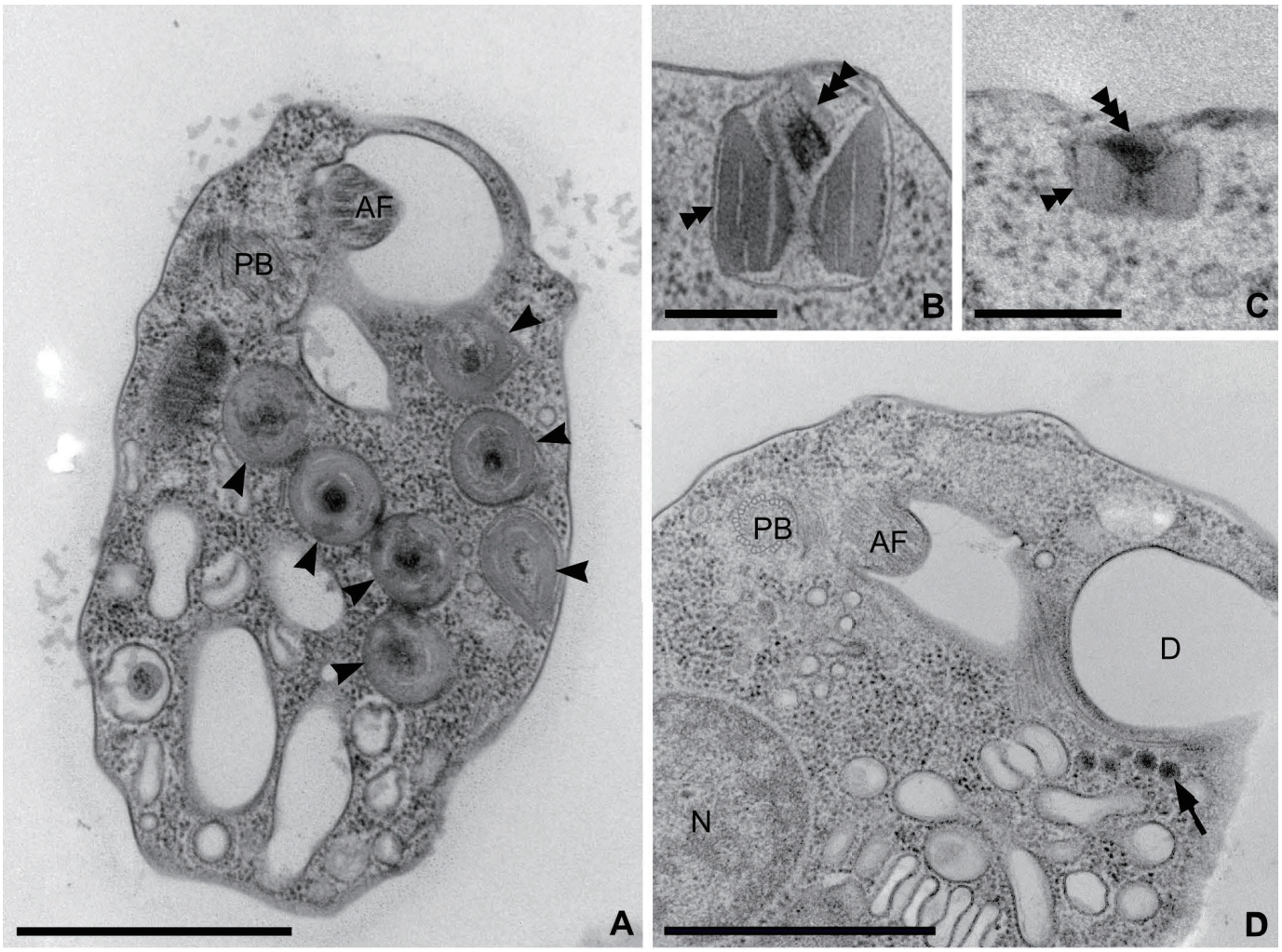

Fig. 6

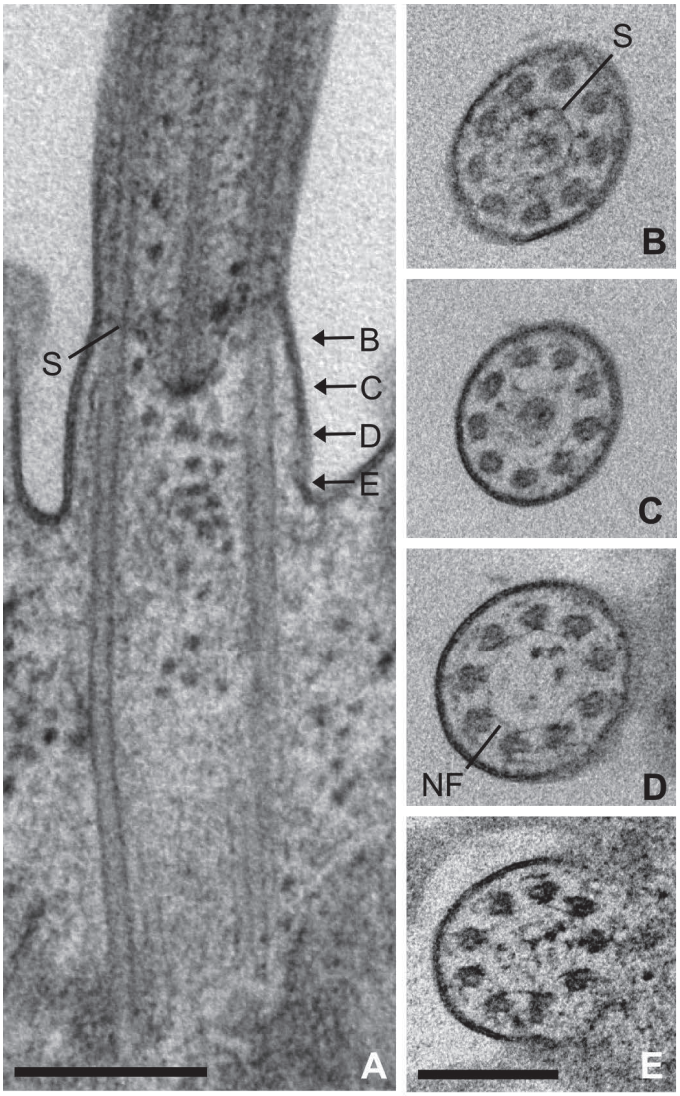

Fig. 7

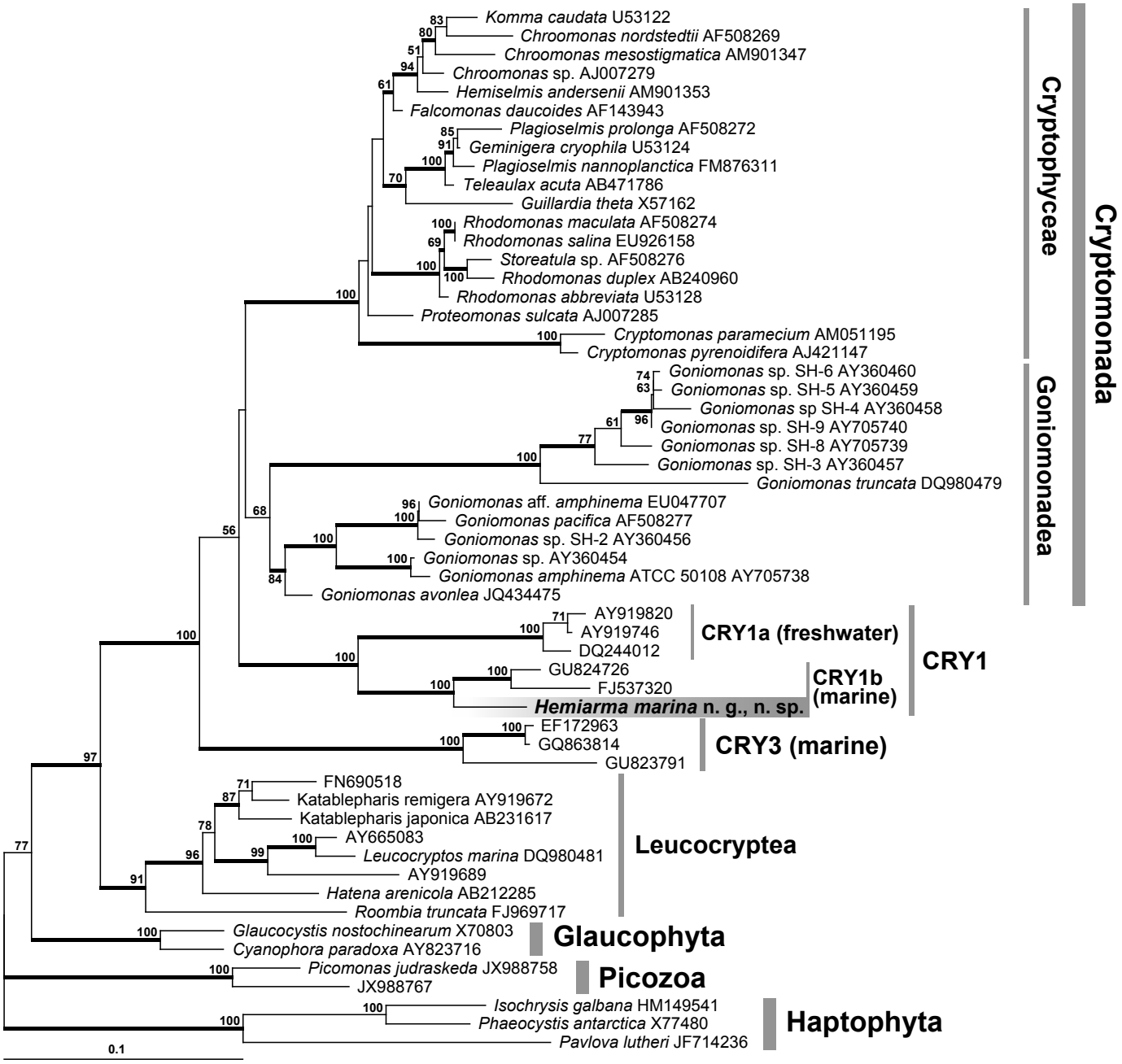
Komma caudata U53122
Chroomonas nordstedtii AF508269
Chroomonas mesostigmatica AM901347
Chroomonas sp. AJ007279
Hemiselmis andersenii AM901353
Falcomonas daucoides AF143943
Plagioselmis prolonga AF508272
Geminigera cryophila U53124
Plagioselmis nannoplanctica FM876311
Teleaulax acuta AB471786
Guillardia theta X57162
Rhodomonas maculata AF508274
Rhodomonas salina EU926158
Storeatula sp. AF508276
Rhodomonas duplex AB240960
Rhodomonas abbreviata U53128
Proteomonas sulcata AJ007285
Cryptomonas paramecium AM051195
Cryptomonas pyrenoidifera AJ421147
Goniomonas sp. SH-6 AY360460
Goniomonas sp. SH-5 AY360459
Goniomonas sp SH-4 AY360458
Goniomonas sp. SH-9 AY705740
Goniomonas sp. SH-8 AY705739
Goniomonas sp. SH-3 AY360457
Goniomonas truncata DQ980479
Goniomonas aff. amphinema EU047707
Goniomonas pacifica AF508277
Goniomonas sp. SH-2 AY360456
Goniomonas sp. AY360454
Goniomonas amphinema ATCC 50108 AY705738
Goniomonas avonlea JQ434475
AY919820
AY919746
DQ244012
CRY1a (freshwater)
GU824726
FJ537320
CRY1b (marine)
Hemiarma marina n. g., n. sp.
CRY1
EF172963
GQ863814
GU823791
CRY3 (marine)
FN690518
Katablepharis remigera AY919672
Katablepharis japonica AB231617
AY665083
Leucocryptos marina DQ980481
AY919689
Hatena arenicola AB212285
Roombia truncata FJ969717
Leucocryptea
Glaucocystis nostochinearum X70803
Cyanophora paradoxa AY823716
Glaucophyta
Picomonas judraskeda JX988758
JX988767
Picozoa
Isochrysis galbana HM149541
Phaeocystis antarctica X77480
Pavlova lutheri JF714236
Haptophyta
0.1
Cryptophyceae
Goniomonadea
Cryptomonada

Fig. 8

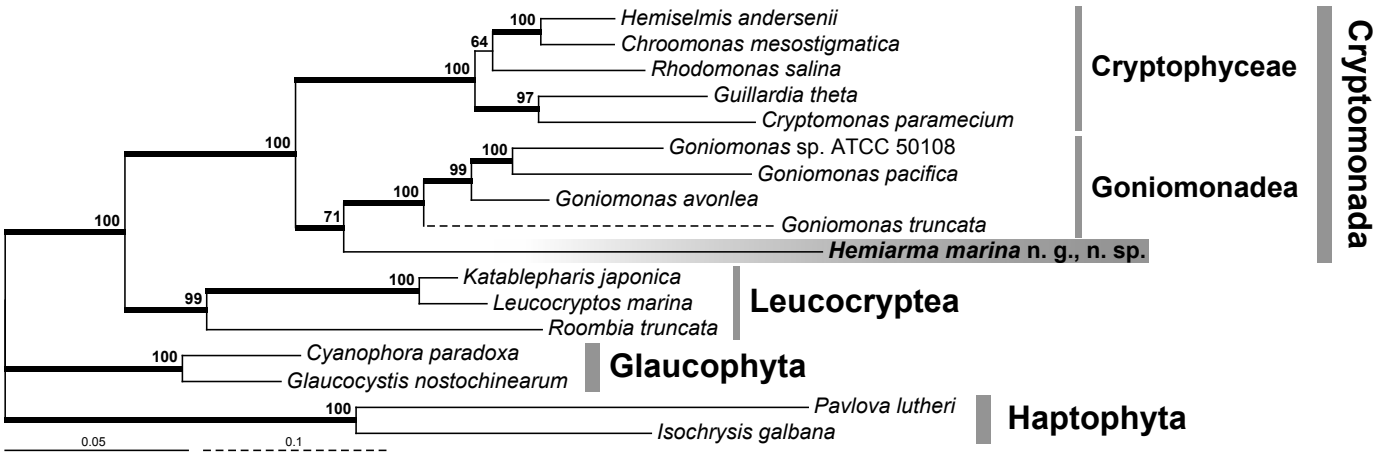
Hemiselmis andersenii
Chroomonas mesostigmatica
Rhodomonas salina
Guillardia theta
Cryptomonas paramecium
Goniomonas sp. ATCC 50108
Goniomonas pacifica
Goniomonas avonlea
Goniomonas truncata
Hemiarma marina n. g., n. sp.
Katablepharis japonica
Leucocryptos marina
Roombia truncata
Cyanophora paradoxa
Glaucocystis nostochinearum
Pavlova lutheri
Isochrysis galbana
100
64
100
97
100
100
99
100
71
100
100
99
100
100
100
0.05
0.1
Cryptophyceae
Goniomonadea
Cryptomonada
Leucocryptea
Glaucophyta
Haptophyta